ACS APPLIED MATERIALS & INTERFACES

Research Article

www.acsami.org

Interphase Evolution of a Lithium-Ion/Oxygen Battery

Giuseppe Antonio Elia,[†] Dominic Bresser,[‡,§,∥] Jakub Reiter,[⊥] Philipp Oberhumer,[⊥] Yang-Kook Sun,[#] Bruno Scrosati,[g] Stefano Passerini,*[,‡,§] and Jusef Hassoun*[,†,h]

[†]Chemistry Department, University of Rome−La Sapienza, Piazzale Aldo Moro 5, 00185 Rome, Italy

[‡]Electrochemistry I, Helmholtz Institute Ulm (HIU), Helmholtzstrasse 11, 89081 Ulm, Germany

[§]Karlsruher Institute of Technology (KIT), P.O. Box 3640, 76021 Karlsruhe, Germany

[∥]INAC/SPRAM/PCI, CEA Grenoble, UMR-5819, CEA-CNRS-UJF, 17 Rue de Martyrs, 38054 Grenoble, Cedex 9, France

[⊥]BMW Group, Petuelring 130, 80788 Munich, Germany

[#]Department of Energy Engineering, Hanyang University, Seoul 133-791, South Korea

[g]Elettrochimica ed Energia, 00199 Rome, Italy

[h]Dipartimento di Scienze Chimiche e Farmaceutiche, Università di Ferrara, Via Fossato di Mortara 17, 44121 Ferrara, Italy

Supporting Information

ABSTRACT: A novel lithium-ion/oxygen battery employing $Pyr_{14}TFSI$-LiTFSI as the electrolyte and nanostructured Li_xSn−C as the anode is reported. The remarkable energy content of the oxygen cathode, the replacement of the lithium metal anode by a nanostructured stable lithium-alloying composite, and the concomitant use of nonflammable ionic liquid-based electrolyte result in a new and intrinsically safer energy storage system. The lithium-ion/oxygen battery delivers a stable capacity of 500 mAh g^{-1} at a working voltage of 2.4 V with a low charge−discharge polarization. However, further characterization of this new system by electrochemical impedance spectroscopy, scanning electron microscopy, and energy-dispersive X-ray spectroscopy reveals the progressive decrease of the battery working voltage, because of the crossover of oxygen through the electrolyte and its direct reaction with the Li_xSn−C anode.

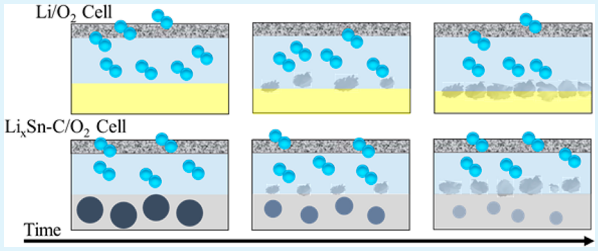

KEYWORDS: *Li/O_2, lithium-ion battery, ionic liquid electrolyte, high efficiency, safety*

INTRODUCTION

The perspective to develop high-energy-density batteries, improving the driving range of electrically powered vehicles to values comparable to those of vehicles powered by conventional combustion engines, has triggered continuously increasing, worldwide research efforts toward the lithium/oxygen system. Indeed, this system provides, in principle, a theoretical energy density comparable to that of fossil fuels.[1,2] The underlying electrochemical process involves the reduction of elemental oxygen and the concomitant, reversible formation and dissolution of lithium peroxide (reaction 1):[3,4]

$$2Li^+ + 2e^- + O_2 \leftrightharpoons Li_2O_2 \quad (1)$$

Conventional lithium/oxygen batteries comprising organic electrolytes combine a lithium metal anode and a carbon-based cathode, the latter operating as electronically conductive support for the electrodeposition of lithium peroxide.[5] However, this configuration provides several drawbacks, which limit the practical application of such battery technology. Besides the potential issues related to the employment of common carbon electrodes at the cathode side,[6−9] one of the main challenges is certainly the poor chemical and electrochemical stability of conventional electrolytes toward the intermediately formed $O_2^{-\bullet}$ superoxide anion radical. This reaction leads to continuous electrolyte degradation and increasing cell polarization, low energy efficiency, and, finally, limited cycle life.[10−15] A variety of electrolyte media, including glymes, ethers, or dimethyl sulfoxide, has been studied,[16,17] with particular interest devoted to ionic liquids (ILs).[17−23] $Pyr_{14}TFSI$, for instance, seems to be a suitable electrolyte medium, allowing very good cycle life and, in particular, outstanding energy storage efficiency.[19,22,23] The stability of this electrolyte medium allowed very good cycling performances,[19,22,23] although with possible side reaction.[24] Indeed, the recent paper of Das et al.[25] compared $Pyr_{14}TFSI$ with 1,2-dimethoxyethane (DME), which is conventionally employed in the lithium−oxygen system, evidencing for the IL better performances and minor ratio of parasitic processes, in particular, for working potential lower than 3.15 V. Furthermore, $Pyr_{14}TFSI$ revealed remarkable compatibility with the common binders (e.g., PVdF), as well as with the carbon substrates used in the Li−air battery. In fact, the already

Received: August 11, 2015
Accepted: September 21, 2015
Published: September 21, 2015

DOI: 10.1021/acsami.5b07414
ACS Appl. Mater. Interfaces 2015, 7, 22638−22643

observed oxidative degradation of cell components, particularly concerning the carbon-based oxygen cathode,[6,9] is presumably favored by the commonly recorded rather high charge potentials, i.e., under conditions that are well avoided when employing IL-based electrolytes due to the substantially lowered polarization.[23]

Besides the electrolyte, an additional challenge toward the commercialization of the lithium−oxygen system is related to the employment of metallic lithium as the anode, which provides severe safety issues, such as the formation of dendrites upon cycling, resulting in a short circuit, consequently leading to a thermal runaway. The safety concerns regarding the utilization of metallic lithium as anode material are, in fact, particularly an issue for the development of lithium−oxygen batteries, considering that these batteries are principally supposed to operate in an ambient atmosphere. Hence, the risks related to the high reactivity of lithium toward moisture and oxygen is even more pronounced in such open systems.

Moreover, the crossover of oxygen from the cathode through the electrolyte to the anode results in substantial self-discharge, additional side reactions, and, finally, rapid fading of the cell.[26,27] Indeed, the oxygen solubilized within the electrolyte may directly react with the lithium metal anode, thus forming lithium oxide species and, in the presence of water traces, lithium hydroxide.[26,27] Hence, the replacement of reactive, metallic lithium by an alternative, safe anode material is considered to enable further enhancement of the lithium/oxygen cell.[28−30]

Herein, we report a lithium-ion/oxygen cell using a nanostructured, lithiated tin−carbon composite as an alternative anode material and a highly stable ionic liquid-based electrolyte, promising substantially enhanced safety. The Sn−C anode material, lithiated prior to use in cell, is formed by a bulk, micrometric carbon matrix trapping metallic tin nanoparticles (10−50 nm).[31] This particular morphology allows an efficient buffering of the occurring volume changes upon (de-)alloying, because of the available free volume within the carbonaceous matrix. This composite design greatly enhances the mechanical stability of the active material and prevents electrode pulverization and consequent cell failure upon cycling. In addition, confining the tin nanoparticles in a micrometric carbon matrix results in the formation of a stabilized SEI at the electrode/electrolyte interface.[31] Furthermore, the Pyr_{14}TFSI−LiTFSI electrolyte, characterized by high thermal stability and compatibility with the lithium−oxygen electrochemical process, allows contemporary high safety and remarkable energy efficiency.[23] Previous papers demonstrated the reversibility of both oxygen cathode and Li−Sn−C anode.[18−23,30,31] Accordingly, the electrochemical process at the cathode has been deeply studied in ILs[18] and other electrolyte media via several techniques, including *ex situ* X-ray photoemission spectroscopy (XPS), scanning electron microscopy (SEM), transmission electron microscopy (TEM), and time-of-flight secondary ion mass spectrometry (TOF−SIMS).[16,23] These papers have clearly proven the reversible formation and dissolution of lithium peroxide. Furthermore, the data evidenced that minor side reactions cannot be excluded. The good reversibility and stability revealed in our works, in contrast to some literature evidence,[10] has been also demonstrated by several groups.[18−23] The good lithium−oxygen battery behavior may be partially attributed to an optimized cell configuration and cycling conditions including cell geometry, gas diffusion layer, and limiting capacity regimes. In the present work, we focused the attention on the replacement of the lithium metal by an alloy-based anode as an important step for the development of a safe lithium oxygen cell. The new energy storage device reported herein was studied, with regard to its electrochemical properties, with a particular focus on the oxygen crossover phenomenon from the cathode to the anode side and its effect on the cell during operation. Scanning electron microscopy (SEM) and energy-dispersive X-ray spectroscopy (EDX), performed both on partially lithiated Sn−C anode and, for comparison, metallic lithium, collected from lithium(-ion)/oxygen cells, clearly indicate the direct reaction of lithium "stored" in the anode and the oxygen dissolved within the electrolyte.

EXPERIMENTAL SECTION

The electrolyte solution was prepared by dissolving 0.2 mol kg^{-1} of lithium bis(trifluoromethanesulfonyl)imide (LiTFSI) in the IL *N*-butyl-*N*-methyl pyrrolidinium bis(trifluoromethanesulfonyl)imide (Pyr_{14}TFSI). The IL was synthesized following a procedure described in detail elsewhere[32,33] and dried under vacuum at 90 °C until a water content of <5 ppm was achieved, as determined by Karl Fischer titration. The oxygen cathode was prepared by coating a slurry of SP-C65 (Imerys) and PVdF (6020 Solef Solvay, as binder) in an 8:2 weight ratio, dispersed in *N*-methyl-2-pyrrolidone (NMP, Aldrich), on a conventional carbon-based gas diffusion layer. The cathode, dried at 110 °C under vacuum for 3 h, had a final SP-C65 loading ranging from 0.5 mg cm^{-2} to 0.8 mg cm^{-2}. The Sn−C nanocomposite-based anode was prepared by thermal treatment of a resorcinol formaldehyde gel impregnated with a tin organometallic precursor in a H_2/Ar (4% H_2) atmosphere, as described in a previous study.[31] The Sn−C composite was comprised of 35 wt % Sn and 65 wt % C, as determined by thermogravimetric analysis (TGA). Accordingly, the theoretical capacity was estimated to be ∼420 mAh g^{-1}, considering the final alloying product $Li_{4.4}Sn$. The Sn−C-based electrodes were prepared by casting a slurry composed of the active material (Sn−C), SP-C65 (Imerys), and PVdF(6020 Solef Solvay, as binder) in an 8:1:1 weight ratio, dispersed in NMP (Aldrich), on copper foil (thickness of 25 μm), serving as a current collector. The average mass loading was in the range of 4−5 mg cm^{-2}. Prior to the electrochemical studies, the Sn−C electrodes were prelithiated to form a Li_xSn−C alloy, with x ranging from 3 to 4, depending on the operating temperature. The prelithiation process, described in detail in a previous manuscript,[34] was performed by setting the electrode directly in contact with metallic lithium, previously wetted with a solution of 1 M $LiPF_6$ in EC:DMC (1:1), applying a pressure of 0.4 kg cm^{-2} for 6 h. The anodes were initially studied in half-cell configuration, employing 2032 coin cells. All studies involving the oxygen cathode were performed using top-meshed 2032 coin cells.[16] Whatman glass felts soaked with the electrolyte were generally employed as separators. Finally, lithium-ion/oxygen full-cells were prepared using a prelithiated Li_xSn−C electrode.

Galvanostatic cycling of Li_xSn−C anodes was carried out by applying a specific current of 50 mA g^{-1} and setting the cutoff potentials to 0.01 and 2.0 V. Lithium/oxygen cells and lithium-ion/oxygen cells were cycled under a capacity-limited regime of 500 mAh g^{-1}, applying a specific current of 50 mA g^{-1}. The specific values of current and capacity are reported with respect to the mass loading of the active material (SP-C65 carbon). All galvanostatic studies were performed by means of a Maccor Series 4000 Battery Test System. The evolution of the open circuit voltage (OCV) and electrochemical impedance spectroscopy (EIS) were carried out utilizing a VMP2/Z multichannel galvanostat-potentiostat (Bio-Logic). EIS was performed in a frequency range from 75 kHz to 0.1 Hz (signal amplitude of 10 mV). *Ex situ* SEM, coupled with energy-dispersive X-ray spectroscopy (EDX), was performed by means of a Zeiss Model Auriga SEM system that was equipped with an EDS detector (INCAPentaFETx3, Oxford Instruments). Prior to the *ex situ* SEM/EDX analysis, the electrodes (including the lithium metal anodes) were rinsed with DMC to remove residual salt and transferred to the SEM system, using a self-

DOI: 10.1021/acsami.5b07414
ACS Appl. Mater. Interfaces 2015, 7, 22638−22643

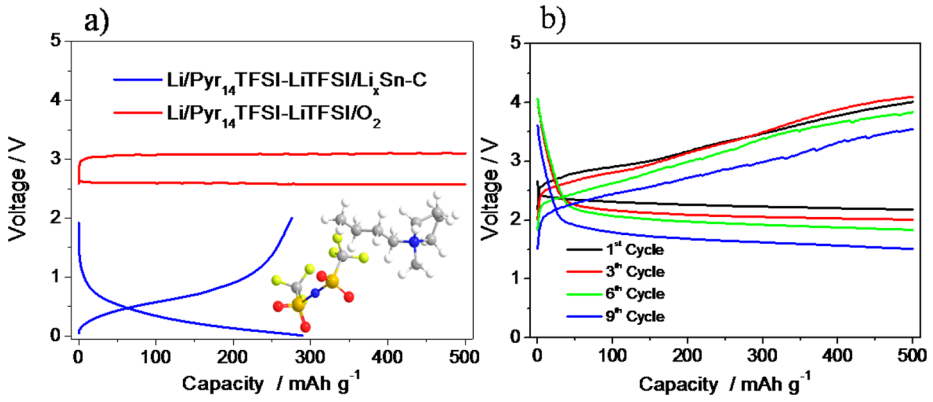

Figure 1. (a) Galvanostatic cycling and the corresponding voltage profiles of Li/Pyr_{14}TFSI−LiTFSI/Li_xSn−C (blue) and Li/Pyr_{14}TFSI−LiTFSI/O_2 (red) half-cells (applied specific current: 50 mA g^{-1}). (b) Galvanostatic cycling and the corresponding voltage profile of a Li_xSn−C/Pyr_{14}TFSI−LiTFSI/O_2 full-cell (specific current: 50 mA g^{-1}), limiting the specific capacity to 500 mAh g^{-1}.

designed sample holder to avoid any exposure of the samples to air and moisture.

RESULTS AND DISCUSSION

Figure 1a reports the voltage profiles of the Li/Li_xSn−C (blue) and the Li/O_2 (red) cells (the inset shows the chemical structure of Pyr_{14}TFSI). The Li_xSn−C electrode delivers a specific capacity of ∼300 mAh g^{-1}, with an average working voltage of ∼0.5 V, showing the expected profile associated with the reversible (de)alloying process of tin and lithium.[31] The lithium/oxygen half-cell shows a reversible (dis)charge profile providing an excellent energy efficiency (i.e., ∼82%), and an average working voltage of ∼2.7 V, as already observed in our previous paper using the Pyr_{14}TFSI−LiTFSI electrolyte.[23] The reversibility of the lithium peroxide formation was illustrated once more by "overcharging" a precisely discharged cell (see Figure S1 in the Supporting Information (SI) section). Apparently, the cell voltage increases rather steeply after a specific capacity of 500 mAh g^{-1}, indicating that, subsequently, other (irreversible) processes occur (for instance, partial electrolyte decomposition), which can be well mitigated when discharging and charging under capacity-limited conditions (see also Figure 1a and ref 23). The voltage profiles of the full-cell, shown in Figure 1b, reflect the combination of the Li_xSn−C anode and the carbon−oxygen cathode signatures, following the electrochemical process described in reaction 2:

$$Li_xSn\text{−}C + \frac{y}{2}O_2 \leftrightharpoons Li_{(x-y)}Sn\text{−}C + \frac{y}{2}Li_2O_2 \qquad (2)$$

The first cycle (Figure1b, black profile) shows an average discharge voltage of ∼2.4 V and a charge voltage centered at 3.2 V. The voltage profile generally appears rather sloped, which is related to the Li/Li_xSn−C alloying process.

Based on the recorded working voltage of 2.4 V and a capacity restricted to 500 mAh g^{-1}, the energy density referred to the mass of the comprised carbon is ∼1200 Wh kg^{-1} (or 1000 Wh kg^{-1}, including the binder), corresponding to a volumetric energy density of 420 Wh L^{-1} (or 335 Wh L^{-1}, including the binder). During the following cycles, the discharge and charge profiles shift to lower voltages,[28] most likely due to the oxygen crossover through the electrolyte and its reaction with the lithiated anode.[26,27] Indeed, the corresponding irreversible consumption of lithium stored within the Li_xSn−C anode provides a reasonable explanation for the observed decrease of the cell voltage. Figure S2 in the SI reports a comparison of the cycling trend of the of the Li/Py_{14}TFSI-LiTFSI/SP-O_2 half-cell and of the Li_xSn−C/Py_{14}TFSI−LiTFSI/SP-O_2 full-cell. The figure shows a stability limited to nine cycles for the full lithium-ion/air cell, and a much higher cycle life for the lithium half-cell.[23]

To further investigate this issue, we recorded the open circuit voltage (OCV) of freshly assembled cells for 12 days. Figure 2

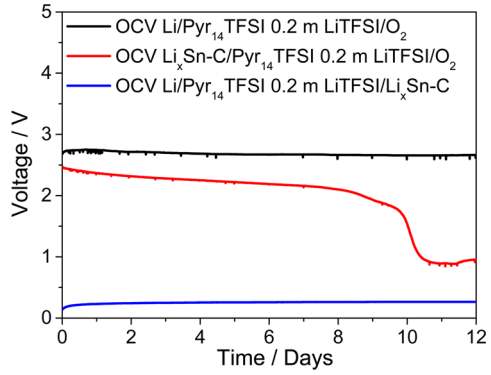

Figure 2. Evolution of the open circuit voltage (OCV) of a Li_xSn−C/Pyr_{14}TFSI−LiTFSI/O_2 (red) full-cell as well as Li/Pyr_{14}TFSI−LiTFSI/O_2 (black) and Li/Pyr_{14}TFSI−LiTFSI/Li_xSn−C (blue, argon atmosphere) half-cells upon 12 days of storage.

shows the OCV evolution of Li_xSn−C/O_2 full-cell (red) and the Li/O_2 half-cell (black) and, for comparison, the OCV recorded for a Li/Li_xSn−C half-cell stored under argon atmosphere (blue). The full-cell shows a slight decay of the OCV within the first 8 days and a subsequent rapid decrease to an OCV of <1 V upon 12 days. This behavior is consistent with the voltage trend observed upon full-cell cycling (Figure 1b) and supports the earlier mentioned assumption, attributing the continuous decrease of the cell voltage to the direct, irreversible reaction of oxygen with the lithiated Sn−C anode resulting in the formation of lithium oxide species.[26,27] The full consumption of the lithium alloyed in the Li_x−Sn-C anode hinders the Li_xSn−C + e^- ⇋ Sn−C + Li^+ redox reaction and, hence, leads to full-cell OCV drop. Instead, the stable OCV trend of the Li_xSn−C half-cell stored under argon (Figure 2, blue curve), excludes the voltage decrease due to electrolyte decomposition. The rather stable OCV of the Li/O_2 cell (Figure 2, black) may be explained by the large lithium excess (i.e., the relatively higher capacity of the lithium metal, with

DOI: 10.1021/acsami.5b07414
ACS Appl. Mater. Interfaces 2015, 7, 22638−22643

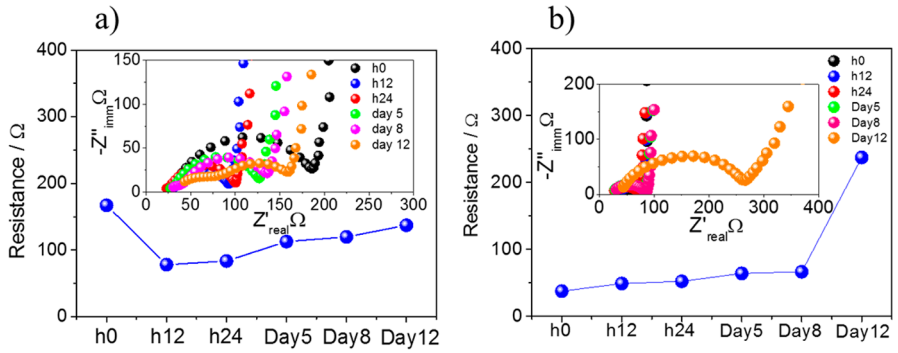

Figure 3. Evolution of the impedance as a function of time for (a) the Li/Pyr_{14}TFSI−LiTFSI/O_2 cell and (b) the Li_xSn−C/Pyr_{14}TFSI−LiTFSI/O_2 cell; the corresponding Nyquist plots are presented as insets.

respect to lithiated Sn−C). Indeed, the Li/O_2 cell comprises 18 mg of metallic lithium, which corresponds to a capacity of ∼72 mAh (i.e., an excess capacity), which efficiently buffers the continuously occurring reaction of lithium and oxygen. However, the total capacity ascribed to Sn−C electrode (mass loading of ∼10 mg) is substantially lower (4 mAh). Accordingly, the Li_xSn−C electrode is more affected by a continuous lithium consumption related to the formation of lithium oxide species at the anode side.[26,27]

These considerations are further supported by the EIS results presented in Figure 3, showing the evolution of the impedance for Li/O_2 (Figure 3a) and Li_xSn−C/O_2 (Figure 3b) cells upon these 12 days of storage under OCV conditions. After an initial stabilization in the case of Li/O_2 (in fact, the SEI on Sn−C is largely formed already during the prelithiation step), both cells show a slight, continuous increase in resistance, indicating the formation of an insulating lithium oxide film at the electrode surface.[26,27] Nevertheless, despite being characterized by lower resistance, most likely due to a different chemistry of the solid electrolyte interphase (SEI), the Li_xSn−C/O_2 cell shows a rapid impedance increase after 8 days of storage under OCV conditions. This trend is in full agreement with the OCV drop upon 8 days of test (compare Figures 2 and 3), thus suggesting the consumption of a substantial amount of lithium stored in the Li_xSn−C anode due to the reaction with solubilized oxygen. Indeed, the recorded cell voltage appears to be largely determined by the lithium oxide species formed at the anode surface, rather than the lithiated Sn−C nanocomposite. A promising strategy to overcome this issue may be the optimization of the SEI and/or the implementation of a protective layer or membrane, preventing the oxygen crossover or at least the reaction of lithium and solubilized oxygen at the anode surface.

The reaction products formed at the anode surface were subsequently studied via *ex situ* SEM, coupled with energy-dispersive X-ray spectroscopy (EDX) analysis (see Figures 4 and 5, respectively). The SEM micrographs presented in Figure 4 reveal a flat and clean surface of the pristine lithium metal (Figure 4a) and the micrometric morphology of the (prelithiated) glassy carbon matrix encapsulating the electrochemically active tin nanoparticles (Figure 4c).[31] After 12 days of storage under an oxygen atmosphere, however, both lithium metal (Figure 4b) and Li_xSn−C (Figure 4d) appear to be covered by large, porous aggregates, revealing a substantial formation of degradation products and the extensive occurrence of side reactions.

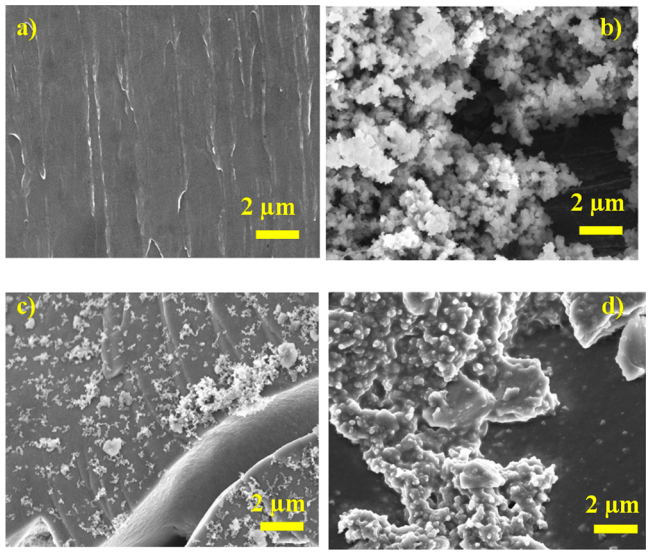

Figure 4. SEM micrographs of (a) a pristine lithium foil; (b) a lithium electrode after 12 days of storage under OCV conditions, assembled in a Li/Pyr_{14}TFSI−LiTFSI/O_2 cell configuration; (c) a pristine, prelithiated Sn−C-based electrode; and (d) a prelithiated Sn−C-based electrode after 12 days of storage under OCV conditions, assembled in a Li_xSn−C/Pyr_{14}TFSI−LiTFSI/O_2 cell configuration.

Figure 5 reports a schematic representation of the reaction occurring at the electrode electrolyte interphase at the OCV, because of the direct reaction of the oxygen solubilized in the electrolyte with the anode material. Lithium metal shows the formation of LiOH or Li_xO_y species at the electrode surface,[27] with consumption of the anode, and the simultaneous formation of a thick film. Instead, Li_xSn−C anode evidences removal of the limited amount of lithium alloyed at the anode side, with the consequent formation of side reaction products, thus leading to a complete consumption of the lithium within a few days of storage under oxygen.

The elemental composition of these degradation products formed at the surface of the Li_xSn−C electrode was investigated by means of EDX analysis (Figure 6). Consistent with the SEM micrograph of Figure 4d, the results clearly evidence an inhomogeneous surface. Parts of the electrode surface (see, e.g., spectrum 6 in Figure 6) are almost clean and mainly composed by carbon with a minor content of oxygen, while other parts of the electrode are covered by porous aggregates (see, e.g., Spectrum 1 in Figure 6) containing a significantly higher amount of oxygen, further confirming the oxidation of the

DOI: 10.1021/acsami.5b07414
ACS Appl. Mater. Interfaces 2015, 7, 22638−22643

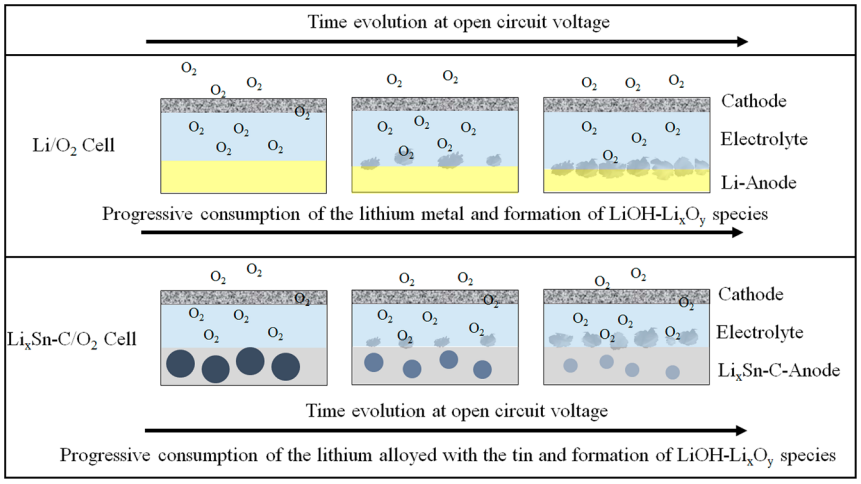

Figure 5. Schematic representation of the reactions occurring at the electrode/electrolyte interphase of the Li/Pyr_{14}TFSI−LiTFSI/O_2 cell and of a Li_xSn−C/Pyr_{14}TFSI−LiTFSI/O_2 cell in the OCV condition, under oxygen atmosphere.

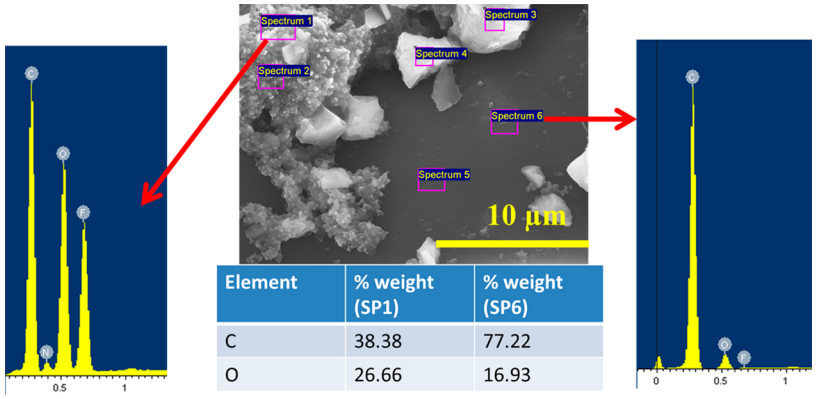

Element	% weight (SP1)	% weight (SP6)
C	38.38	77.22
O	26.66	16.93

Figure 6. SEM micrograph and the results of the EDX analysis of the prelithiated Sn−C-based electrode after 12 days of storage under OCV conditions, assembled in a Li_xSn−C/Pyr_{14}TFSI−LiTFSI/O_2 cell configuration.

electrode, which is consistent with the electrochemical results. The above surface oxidation is expected to produce lithium oxide species, i.e., the same reaction products already observed for the lithium metal electrode in a lithium/oxygen cell.[26,27] Nevertheless, further experiments will certainly be required to obtain a more detailed understanding of the underlying processes.

CONCLUSIONS

The results presented herein confirm the suitability of lithium-ion/oxygen batteries using an IL-based electrolyte and a nanostructured Sn−C anode as a new electrochemical energy storage system. However, galvanostatic cycling as well as electrochemical impedance spectroscopy (EIS), scanning electron microscopy (SEM), and energy-dispersive X-ray (EDX) analyses revealed critical issues associated to the oxygen crossover through the electrolyte followed by its reaction at the anode surface and a consequent deterioration of the cell performance. These results suggest that the direct oxidation of the anode surface and formation of lithium oxide species lead to a continuously decreasing cell voltage upon cycling, as well as upon storage. This issue may be efficiently mitigated both by optimizing the characteristics of the SEI and/or using protective layers or membranes to avoid the undesired side reactions originating from the oxygen crossover.[35,36] Indeed, we are confident that the high energy content and enhanced safety of lithium-ion/oxygen batteries will trigger further research aimed to address the major problems presently affecting this system, finally enabling extended driving ranges for future electric vehicles.

ASSOCIATED CONTENT

Supporting Information

The Supporting Information is available free of charge on the ACS Publications website at DOI: 10.1021/acsami.5b07414.

Voltage profile for a Li/Py_{14}TFSI-LiTFSI/O_2 cell, limiting the discharge capacity to 500 mAh g^{-1} and "overcharging" the cell to a cutoff potential of 4.3 V; comparison of the cycling behavior of the Li/Py_{14}TFSI-LiTFSI/O_2 half-cell and of the Li_xSn−C/Py_{14}TFSI-LiTFSI/O_2 full-cell, limiting the discharge capacity to 500 mAh g^{-1} (PDF)

AUTHOR INFORMATION

Corresponding Authors

*E-mail: stefano.passerini@kit.edu (S. Passerini).
*E-mail: jusef.hassoun@unife.it (J. Hassoun).

Notes

The authors declare no competing financial interest.

DOI: 10.1021/acsami.5b07414
ACS Appl. Mater. Interfaces 2015, 7, 22638−22643

■ ACKNOWLEDGMENTS

This work was financially supported by BMW AG within the ABILE (Air Batteries with Ionic Liquid Electrolytes) project.

■ REFERENCES

(1) Scrosati, B.; Hassoun, J.; Sun, Y. K. Lithium-Ion Batteries. A Look Into the Future. *Energy Environ. Sci.* **2011**, *4*, 3287−3295.
(2) Girishkumar, G.; McCloskey, B.; Luntz, A. C.; Swanson, S.; Wilcke, W. Lithium−Air Battery: Promise and Challenges. *J. Phys. Chem. Lett.* **2010**, *1*, 2193−2203.
(3) Lu, Y. C.; Gallant, B. M.; Kwabi, D. G.; Harding, J. R.; Mitchell, R. R.; Whittingham, M. S.; Shao-Horn, Y. Lithium−Oxygen Batteries: Bridging Mechanistic Understanding and Battery Performance. *Energy Environ. Sci.* **2013**, *6*, 750−768.
(4) Bruce, P. G.; Freunberger, S. A.; Hardwick, L. J.; Tarascon, J. M. Li-O_2 and Li-S Batteries with High Energy Storage. *Nat. Mater.* **2011**, *11*, 19−29.
(5) Abraham, K. M.; Jiang, Z. A Polymer Electrolyte-Based Rechargeable Lithium/Oxygen Battery. *J. Electrochem. Soc.* **1996**, *143*, 1−5.
(6) McCloskey, B. D.; Speidel, A.; Scheffler, R.; Miller, D. C.; Viswanathan, V.; Hummelshøj, J. S.; Nørskov, J. K.; Luntz, A. C. Twin Problems of Interfacial Carbonate Formation in Nonaqueous Li−O_2 Batteries. *J. Phys. Chem. Lett.* **2012**, *3*, 997−1001.
(7) Ottakam Thotiyl, M. M.; Freunberger, S. A.; Peng, Z.; Bruce, P. G. The Carbon Electrode in Nonaqueous Li−O_2 Cells. *J. Am. Chem. Soc.* **2013**, *135*, 494−500.
(8) Ottakam Thotiyl, M. M.; Freunberger, S. A.; Peng, Z.; Chen, Y.; Liu, Z.; Bruce, P. G. A Stable Cathode for the Aprotic Li−O_2 Battery. *Nat. Mater.* **2013**, *12*, 1050−1056.
(9) Black, R.; Oh, S. H.; Lee, J. H.; Yim, T.; Adams, B.; Nazar, L. F. Screening for Superoxide Reactivity in Li-O_2 Batteries: Effect on Li_2O_2/LiOH Crystallization. *J. Am. Chem. Soc.* **2012**, *134*, 2902−2905.
(10) Luntz, A. C.; McCloskey, B. D. Nonaqueous Li−Air Batteries: a Status Report. *Chem. Rev.* **2014**, *114*, 11721−11750.
(11) Grande, L.; Paillard, E.; Hassoun, J.; Park, J. B.; Lee, Y. J.; Sun, Y. K.; Passerini, S.; Scrosati, B. The Lithium/Air Battery: Still an Emerging System or a Practical Reality? *Adv. Mater.* **2015**, *27*, 784−800.
(12) Hassoun, J.; Croce, F.; Armand, M.; Scrosati, B. Investigation of the O_2 Electrochemistry in a Polymer Electrolyte Solid-State Cell. *Angew. Chem., Int. Ed.* **2011**, *50*, 2999−3002.
(13) Freunberger, S. A.; Chen, Y.; Peng, Z.; Griffin, J. M.; Hardwick, L. J.; Bardé, F.; Novák, P.; Bruce, P. G. Reactions in the Rechargeable Lithium−O_2 Battery with Alkyl Carbonate Electrolytes. *J. Am. Chem. Soc.* **2011**, *133*, 8040−8047.
(14) Xu, W.; Viswanathan, V. V.; Wang, D.; Towne, S. A.; Xiao, J.; Nie, Z.; Hu, D.; Zhang, J.-G. Investigation on the Charging Process of Li_2O_2-Based Air Electrodes in Li−O_2 Batteries with Organic Carbonate Electrolytes. *J. Power Sources* **2011**, *196*, 3894−3899.
(15) McCloskey, B. D.; Bethune, D. S.; Shelby, R. M.; Girishkumar, G.; Luntz, A. C. Solvents' Critical Role in Nonaqueous Lithium−Oxygen Battery Electrochemistry. *J. Phys. Chem. Lett.* **2011**, *2*, 1161−1166.
(16) Jung, H. G.; Hassoun, J.; Park, J. B.; Sun, Y. K.; Scrosati, B. An Improved High-Performance Lithium−Air Battery. *Nat. Chem.* **2012**, *4*, 579−585.
(17) Peng, Z.; Freunberger, S. A.; Chen, Y.; Bruce, P. G. A Reversible and Higher-Rate Li-O_2 Battery. *Science* **2012**, *337*, 563−566.
(18) Monaco, S.; Soavi, F.; Mastragostino, M. Role of Oxygen Mass Transport in Rechargeable Li/O_2 Batteries Operating with Ionic Liquids. *J. Phys. Chem. Lett.* **2013**, *4*, 1379−1382.
(19) Bresser, D.; Paillard, E.; Passerini, S. Ionic Liquid-Based Electrolytes for Li Metal/Air Batteries: A Review of Materials and the New 'LABOHR' Flow Cell Concept. *J. Electrochem. Sci. Technol.* **2014**, *5*, 37−44.
(20) Randström, S.; Appetecchi, G. B.; Lagergren, C.; Moreno, A.; Passerini, S. The Influence of Air and Its Components on the Cathodic Stability of *N*-butyl-*N*-methylpyrrolidinium bis-(trifluoromethanesulfonyl)imide. *Electrochim. Acta* **2007**, *53*, 1837−1842.
(21) Jung, K. N.; Lee, J. I.; Jung, J. H.; Shin, K. H.; Lee, J. W. A Quasi-Solid-State Rechargeable Lithium−Oxygen Battery Based on a Gel Polymer Electrolyte with an Ionic Liquid. *Chem. Commun.* **2014**, *50*, 5458−5461.
(22) Soavi, F.; Monaco, S.; Mastragostino, M. Catalyst-Free Porous Carbon Cathode and Ionic Liquid for High Efficiency, Rechargeable Li/O_2 Battery. *J. Power Sources* **2013**, *224*, 115−119.
(23) Elia, G. A.; Hassoun, J.; Kwak, W.-J.; Sun, Y.-K.; Scrosati, B.; Mueller, F.; Bresser, D.; Passerini, S.; Oberhumer, P.; Tsiouvaras, N.; Reiter, J. An Advanced Lithium-Air Battery Exploiting an Ionic Liquid-Based Electrolyte. *Nano Lett.* **2014**, *14*, 6572−6577.
(24) Piana, M.; Wandt, J.; Meini, S.; Buchberger, I.; Tsiouvaras, N.; Gasteiger, H. A. Stability of a Pyrrolidinium-Based Ionic Liquid in Li-O_2 Cells. *J. Electrochem. Soc.* **2014**, *161*, A1992−A2001.
(25) Das, S.; Højberg, J.; Knudsen, K. B.; Younesi, R.; Johansson, P.; Norby, P.; Vegge, T. Instability of Ionic Liquid Based Electrolytes in Li-O_2 Batteries. *J. Phys. Chem. C* **2015**, *119*, 18084−18090.
(26) Assary, R. S.; Lu, J.; Du, P.; Luo, X.; Zhang, X.; Ren, Y.; Curtiss, L. A.; Amine, K. (2013). The Effect of Oxygen Crossover on the Anode of a Li−O_2 Battery using an Ether-Based Solvent: Insights from Experimental and Computational Studies. *ChemSusChem* **2013**, *6*, 51−55.
(27) Shui, J. L.; Okasinski, J. S.; Kenesei, P.; Dobbs, H. A.; Zhao, D.; Almer, J. D.; Liu, D. J. Reversibility of Anodic Lithium in Rechargeable Lithium−Oxygen Batteries. *Nat. Commun.* **2014**, *4*, 2255.
(28) Hassoun, J.; Jung, H. G.; Lee, D. J.; Park, J. B.; Amine, K.; Sun, Y. K.; Scrosati, B. A Metal-Free, Lithium-Ion Oxygen Battery: A Step Forward to Safety in Lithium-Air Batteries. *Nano Lett.* **2012**, *12*, 5775−5779.
(29) Chun, J.; Kim, H.; Jo, C.; Lim, E.; Lee, J.; Kim, Y. Reversibility of Lithium-Ion−Air Batteries Using Lithium Intercalation Compounds as Anodes. *ChemPlusChem* **2015**, *80*, 349−353.
(30) Elia, G. A.; Bernhard, R.; Hassoun, J. A Lithium-Ion Oxygen Battery Using a Polyethylene Glyme Electrolyte Mixed with an Ionic Liquid. *RSC Adv.* **2015**, *5*, 21360−21365.
(31) Derrien, G.; Hassoun, J.; Panero, S.; Scrosati, B. Nanostructured Sn−C Composite as an Advanced Anode Material in High-Performance Lithium-Ion Batteries. *Adv. Mater.* **2007**, *19*, 2336−2340.
(32) Appetecchi, G. B.; Montanino, M.; Zane, D.; Carewska, M.; Alessandrini, F.; Passerini, S. Effect of the Alkyl Group on the Synthesis and the Electrochemical properties of *N*-Alkyl-*N*-methyl-pyrrolidinium bis(trifluoromethanesulfonyl)imide Ionic Liquids. *Electrochim. Acta* **2009**, *54*, 1325−1332.
(33) Appetecchi, G. B.; Scaccia, S.; Tizzani, C.; Alessandrini, F.; Passerini, S. Synthesis of Hydrophobic Ionic Liquids for Electrochemical Applications. *J. Electrochem. Soc.* **2006**, *153*, A1685−A1691.
(34) Hassoun, J.; Lee, K. S.; Sun, Y. K.; Scrosati, B. An Advanced Lithium Ion Battery Based on High Performance Electrode Materials. *J. Am. Chem. Soc.* **2011**, *133*, 3139−3143.
(35) Mizuno, F.; Hayashi, A.; Tadanaga, K.; Tatsumisago, M. New, Highly Ion-Conductive Crystals Precipitated from Li2S−P2S5 Glasses. *Adv. Mater.* **2005**, *17*, 918−921.
(36) Fu, J. *Lithium ion conductive glass-ceramics*, U.S. Patent No. 5,702,995, Dec. 30, 1997.

DOI: 10.1021/acsami.5b07414
ACS Appl. Mater. Interfaces 2015, 7, 22638−22643